Partinen, Jere; Halli, Petteri; Helin, Sampsa; Wilson, Benjamin P.; Lundström, Mari

Utilizing Cu$^+$ as catalyst in reductive leaching of lithium-ion battery cathode materials in H$_2$SO$_4$–NaCl solutions

Utilizing Cu$^+$ as catalyst in reductive leaching of lithium-ion battery cathode materials in H$_2$SO$_4$–NaCl solutions

Jere Partinen, Petteri Halli, Sampsa Helin, Benjamin P. Wilson, Mari Lundström [*]

Aalto University, School of Chemical Engineering, Department of Chemical and Metallurgical Engineering, 00076 Aalto, Finland

A B S T R A C T

In this study, we introduce a novel waste battery leaching system that utilizes elemental copper both as a reductant and catalyst in a sulfuric acid-based lixiviant. Adding chloride ions into the solution stabilizes Cu$^+$ species as complexes, which facilitates their use as catalysts for electron transfer between LiCoO$_2$ and copper. With this leaching system, Co, and Li dissolutions of over 90% were achieved within two hours under mild conditions (1 M H$_2$SO$_4$, 0.2 M NaCl, and 30 °C), thereby avoiding the use of high temperatures, concentrated acids, and external reductants – like H$_2$O$_2$ – that are commonly utilized in battery recycling studies. The XRD analyses of leach residues showed that Cu dissolution proceeded via an intermediate step where solid CuCl precipitated on the surface of Cu, inhibiting the dissolution of both Cu and LiCoO$_2$. The detrimental effects of CuCl precipitation were avoided by increasing the chloride concentration to $\geq$1.6 M, which allowed for very fast leaching kinetics (reaction rates up to $k_c = 21.8 \times 10^{-3}$ min^{-1}). However, such high chloride concentrations also significantly increased the Cu consumption and decreased its reductive efficiency.

1. Introduction

The ongoing transition from fossil fuel-based to renewable power sources has dramatically increased the demand of batteries for energy storage. As the electrification of societies progresses, an increasing number of batteries – especially lithium-ion batteries (LIBs) – will be needed both in transportation and stationary energy storage applications. With this growth in LIBs utilization, there is also a parallel rise in the demand for the essential related component metals and materials (European Commission, 2021). For example, the annual cobalt demand for electric vehicle batteries is expected to rise from 19,000 t (in 2019) to 180,000–370,000 t, and lithium demand from 17,000 to 190,000–370,000 t by 2030 (IEA, 2020). Due to their economic importance and supply risk – resulting from a lack of available resources within Europe and global geo-political concerns – cobalt and lithium have been listed as critical raw materials by the European Commission (Blengini et al., 2020). Consequently, there has been significant focus on the importance of efficient and more sustainable recycling processes for spent battery wastes to enhance the recovery of their valuable metals content for reuse.

Many different methodologies have been investigated for recycling lithium-ion batteries, including pyrometallurgical, hydrometallurgical, and direct physical recycling techniques, along with various pretreatment procedures (Ordoñez et al., 2016; Zhang et al., 2018; Harper et al., 2019). Of the approaches listed, hydrometallurgical recycling methods are considered the most promising due to their advantages over pyrometallurgical routes, such as higher selectivity and recovery, milder reaction conditions, and lower emissions (Lv et al., 2018a; Zhang et al., 2018). Hydrometallurgical recycling entails leaching the desired metals from the battery waste and using solvent extraction and precipitation to subsequently recover the metals from the leach solution (Harper et al., 2019).

Although, leaching of lithium-ion batteries has been previously investigated in a wide range of lixiviants – including hydrochloric acid, ammonia, citric acid, and oxalic acid (Lv et al., 2018a; Yao et al., 2018) – sulfuric acid remains the most investigated lixiviant due to its widespread industrial use (Harper et al., 2019). Nan et al. (2005) were among the first to propose a mechanism for the reaction between sulfuric acid and LiCoO$_2$ (LCO), Eq. 1.

$$4LiCoO_2(s) + 6H_2SO_4(aq) \rightarrow 2Li_2SO_4(aq) + 4CoSO_4(aq) + O_2(g) + 6H_2O(l)$$
(1)
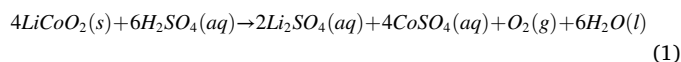
Typically, only around 40% of Co can be leached with sulfuric acid alone, and this has been attributed to the formation of Co$_3$O$_4$ (Eq. 2) that

---

* Corresponding author.
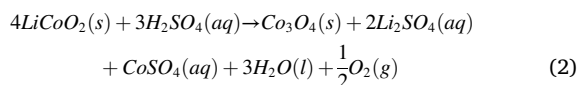 *E-mail address:* mari.lundstrom@aalto.fi (M. Lundström).

can significantly reduce the dissolution reaction rate (Ferreira et al., 2009). To achieve higher leaching efficiencies, a wide variety of chemicals have been studied as possible beneficial reductants, ranging from H_2O_2 (Sohn et al., 2006), Na_2SO_3 (Zheng et al., 2017), NH_4Cl (Lv et al., 2018b), glucose, sucrose, cellulose (Chen et al., 2018), tea waste (Chen et al., 2019), to NiMH battery waste (Liu et al., 2019).

$$4LiCoO_2(s) + 3H_2SO_4(aq) \rightarrow Co_3O_4(s) + 2Li_2SO_4(aq)$$
$$+ CoSO_4(aq) + 3H_2O(l) + \frac{1}{2}O_2(g) \quad (2)$$

One alternative approach to the addition of reductants for LIB leaching is to utilize the metallic fragments typically present within the battery waste itself. For example, Peng et al. (2019) have used mixed Cu and Al current collector foils from industrial battery waste as reductants, whereas Joulié et al. (2017) and Chernyaev et al. (2021) have studied the reductive capabilities of these metals separately. Additionally, Porvali et al. (2020a) investigated a sulfuric acid-based leaching system where the LIB active material reduction was catalyzed by ferrous (Fe^{2+}) ions, with the resulting ferric (Fe^{3+}) ions reduced back to ferrous state by the presence of metallic Cu. In this system, the Fe^{2+}/Fe^{3+} ions facilitate the electron transfer between Cu and $LiCoO_2$, as Cu alone cannot act as a reductant due to the instability of the Cu^+ ion in aqueous and sulfate media (Greenwood and Earnshaw, 1997). The findings demonstrated that the Fe^{2+}/Fe^{3+} ion pair acts as an efficient electron transfer catalyst between LCO and Cu, which allows high Co leaching efficiencies (> 90%) to be achieved even at relatively low dissolved iron concentrations (~1 g/L) (Porvali et al., 2020a). From the results it could be concluded that the factors limiting the rate of LCO dissolution in the leaching system were the reactions between Fe^{3+} and Cu rather than those between Fe^{2+} and LCO. A subsequent study based on the same leaching system showed that Co dissolution yields of 92% were also possible under conditions of low acidity (0.34 M) and temperature (30 °C) (Porvali et al., 2020b).

On the other hand, the addition of complexing ions such as Cl^- into the system may provide an alternative and potentially iron-free catalyzing route between Cu and LCO. Chloride ions stabilize the monovalent copper as chloride complexes, enabling electron transfer between the two reactants. The speciation of Cu^+ depends on the chloride concentration of the solution so that the $[CuCl_2]^-$ complex becomes stable at around 0.02 M and is the prevailing species at low Cl^- concentrations, whereas $[CuCl_3]^{2-}$ becomes dominant at approximately 1–1.5 M Cl^-, and at even higher concentrations, $[CuCl_4]^{3-}$ is also formed (Fritz, 1980; Muir, 2002; Lundström et al., 2005; Senanayake, 2007). Moreover, the Cu^{2+} ion can also form complexes with chloride ions, existing primarily in the form of hydrated Cu^{2+} in dilute chloride solutions, whereas increasing the chloride concentration promotes formation of complexes such as $[CuCl]^+$ and $[CuCl_2]^0$ (Zhao et al., 2013). Table 1 lists the reduction potentials of different half-cell reactions relevant to LCO leaching in the presence of H_2SO_4, Cl^- ions, and Cu. As can be seen, the reductive power of dissolved monovalent copper changes depending on the predominant chloride complex species (i.e., as a function of Cl^- concentration). However, it is also clear that the potential reductive power available is higher when compared to previously studied reductants H_2O_2 or Fe^{2+}/Fe^{3+}. Although, the reduction potential of the Fe^{2+}/Fe^{3+} ion pair also changes with variation of the chloride concentration in the solution, this potential only decreases below that of the Cu^+/Cu^{2+} pair at concentrations above 3 M Cl^- (Muir, 2002).

The Cu^+/Cu^{2+} system has previously been utilized in several leaching applications, including chalcopyrite (Lundström et al., 2005), chalcocite (Hashemzadeh et al., 2019), copper flatpacks (Herreros et al., 2005), and gold (Seisko et al., 2019). However, all these applications use Cu^{2+} as an oxidant, exploiting the tendency of the resulting Cu^+ ion to oxidize back to Cu^{2+} by oxygen gas (Eq. 11). Conversely, such a characteristic could be detrimental to a system using monovalent copper as a catalyst in LCO leaching, as the presence of atmospheric oxygen can readily oxidize the monovalent copper to Cu^{2+}, thus decreasing the catalyst efficiency and increasing Cu consumption.

$$4Cu^+(aq) + O_2(g) + 4H^+(aq) \rightarrow 4Cu^{2+}(aq) + 2H_2O(l) \quad (11)$$
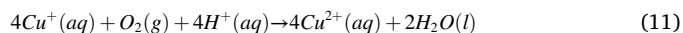
Compared to ferrous ions, the advantage of using cuprous chloride complexes as catalysts in waste battery leaching is that the Cu content of the scrap is typically much higher than Fe (Peng et al., 2019; Porvali et al., 2019). Therefore, the system does not need to rely on the iron content of the waste to enable electron transfer between Cu and LCO. Additionally, the required Cl^- content can be supplied in the form of an inexpensive salt like NaCl. The LIB waste leaching has been previously studied in acidic chloride media, especially in HCl, which is typically chosen due to its intrinsic ability to act as a reductant towards battery cathode materials (Takacova et al., 2016; Porvali et al., 2019). Nevertheless, these studies often attribute the reductive efficiency of HCl to the formation of Cl_2 gas (Eq. 12), meaning that the possible effects of impurity metals like Cu in the presence of chloride ions are often neglected.

$$2LiCoO_2(s) + 8HCl(aq) \rightarrow 2LiCl(aq) + 2CoCl_2(aq) + Cl_2(g) + 4H_2O(l) \quad (12)$$
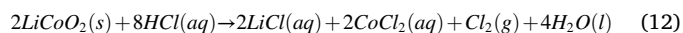
The aim of this study is to investigate the role of complexed monovalent copper species as catalysts in reductive LCO leaching and the effect of chloride concentration on enabling their utilization in sulfuric acid solutions.

2. Materials and methods

The following chemicals were used in this investigation: sulfuric acid (0.5 M and 1.0 M, prepared from 95 to 97% H_2SO_4, VWR Chemicals, Belgium), lithium cobalt oxide (> 99.5% $LiCoO_2$, 5 μm APS powder, Alfa Aesar, Germany), copper powder (99.5% Cu, < 425 μm, Sigma-Aldrich, USA) and sodium chloride (≥ 98% NaCl, VWR Chemicals, Belgium).

Leaching experiments were performed in a 500 mL round-bottom glass-jacketed reactor (OM Lasilaite Oy, Finland) with agitation (VOS 16, VWR, USA, equipped with a four-blade 5 cm diameter PTFE (polytetrafluoroethylene) agitator with 45° blade angle) to keep the reactants in suspension. Experiments were performed in batches of 400 mL at a temperature of 30 °C, which was regulated with a circulating water bath (Lauda A100 Germany). Each experiment used 6.85 g (0.07 mol) of pure $LiCoO_2$ and 4.45 g (0.07 mol) of Cu powder, resulting in a 1 mol/mol ratio of $Cu/LiCoO_2$. Chloride ions were added in the form of sodium chloride, which was dissolved into the lixiviant before starting each experiment. All the solutions were prepared with Milli-Q (Merck, France) ion exchanged water (15.0 MΩ cm). To minimize the effect of dissolved atmospheric oxygen, nitrogen (industrial grade, Linde, Finland) was sparged through the stirred solution for 10 min prior to the addition of solid reactants and this was maintained throughout the whole experimental procedure. The flow rate of nitrogen was regulated at a rate of 0.5 L/min with a calibrated rotameter (LH-ZC51-HR, Kytölä, Finland).

The leaching series consisted of 14 experiments in which the

Table 1
Reduction reactions and their potentials calculated at 30 °C using HSC 9.4.1 (Metso Outotec, 2018).

Half cell reaction	E vs. SHE (V)	Reaction no.
$LiCoO_2(s) + 4H^+(aq) + e^- \rightarrow Li^+(aq) + Co^{2+}(aq) + 2H_2O(l)$	2.152	(3)
$O_2(g) + 2H^+(aq) + 2e^- \rightarrow H_2O_2(l)$	0.619	(4)
$Cu^{2+}(aq) + 2e^- \rightarrow Cu(s)$	0.337	(5)
$Cu^{2+}(aq) + e^- \rightarrow Cu^+$	0.160	(6)
$Cu^{2+}(aq) + 2Cl^-(aq) + e^- \rightarrow CuCl_2^-(aq)$	0.486	(7)
$CuCl^+(aq) + 2Cl^-(aq) + e^- \rightarrow CuCl_3^{2-}(aq)$	0.418	(8)
$CuCl^+(aq) + 3Cl^-(aq) + e^- \rightarrow CuCl_4^{3-}(aq)$	0.295	(9)
$Fe^{3+}(aq) + e^- \rightarrow Fe^{2+}(aq)$	0.644	(10)

concentrations of sulfuric acid (0.5 M and 1.0 M) and NaCl (0–3.2 M) were varied. Total leaching time in each experiment was 2 h, and sampling was performed at 5, 15, 30, 45, 60, 90, and 120 min by retrieving 6 mL of solution from the reactor. Additionally, a redox electrode (Ag/AgCl 3 M KCl, InLab, Mettler Toledo, USA) attached to a multimeter (Fluke 77 IV, USA) was used to monitor the in-situ redox potential. All samples were filtered through 0.45 μm polyethersulfone syringe filters (VWR, USA). The elements of interest (Co, Li, Cu) were analyzed from the solution samples with AAS (atomic absorption spectroscopy, Thermo Scientific iCE 3000, USA), and the pregnant leach solution (PLS) was filtered with a Büchner funnel equipped with Whatman grade 50 filter paper (UK). Leach residues were dried overnight in an oven at 60 °C and analyzed with XRD (X-ray diffraction, PANalytical X'PERT Powder PRO, PIXcel1D detector, Cu Kα source operated at 45 kV, 40 mA along with Fe beta filter and no monochromator, and HighScore PLUS software, the Netherlands).

3. Results and discussion

3.1. LCO leaching as a function of NaCl and H2SO4 concentration

In the absence of chloride ions, sulfuric acid solution was able to dissolve only 38–40% of Co and 66–68% of Li in 2 h (Fig. 1). Although, the reduction agent – elemental Cu – was present in the system, the low leaching efficiency of Co resulted from a lack of an available catalytic species (Cu^+) capable of transferring electrons from Cu to LCO. Moreover, the overall instability of the Cu^+ ion in aqueous and sulfate media

ensures that any cuprous ion generated in solution is short-lived (Greenwood and Earnshaw, 1997). In contrast, the higher level of Li dissolution observed in the absence of chlorides results from delithiation, a known dissolution mechanism of LCO, which proceeds via the release of Li-atoms from the crystal structure (Takacova et al., 2016).

Nevertheless, it is clear from Fig. 1A and C (at 1 M H_2SO_4) that even a minor NaCl addition (0.1 M) proved to be sufficient to stabilize the monovalent copper species in the solution. This stability enabled efficient electron transfer from elemental Cu to LCO to occur, which resulted in the improved dissolution of both Co (65%) and Li (73%). An increase of the NaCl concentration to 0.2 M enhanced the dissolution of both metals (91% Co, 91% Li), however, further intermediate additions (0.4 M and 0.8 M) had only minor impacts on the dissolution rate and final leaching efficiencies. In contrast, further increases in the NaCl concentration within the lixiviant solution to 1.6 M and 3.2 M led to a drastic rise in leaching kinetics with almost complete dissolution of LCO achieved after only 30 min. Depletion of LCO was also reflected by the solution redox potential, which decreased rapidly after most of the LCO had dissolved (Fig. S1). With 0.5 M H_2SO_4 (Fig. 1B and D), the chloride concentration of the solution had similar effects as with 1 M H_2SO_4, although overall, the leaching efficiencies were generally less at the lower level of acidity. Additionally, notable increases in kinetics were observed at two NaCl concentrations: first at 0.8 M, increasing the final dissolved fraction of Co from 73% to 97%, and later at 3.2 M, reaching almost complete dissolution in 45 min. The simplified reaction between the reactants – shown in Eq. 13 – involves the dissolution of LCO into the solution as the Cu^+ species oxidize to Cu^{2+}. Moreover, the resulting Cu^{2+}
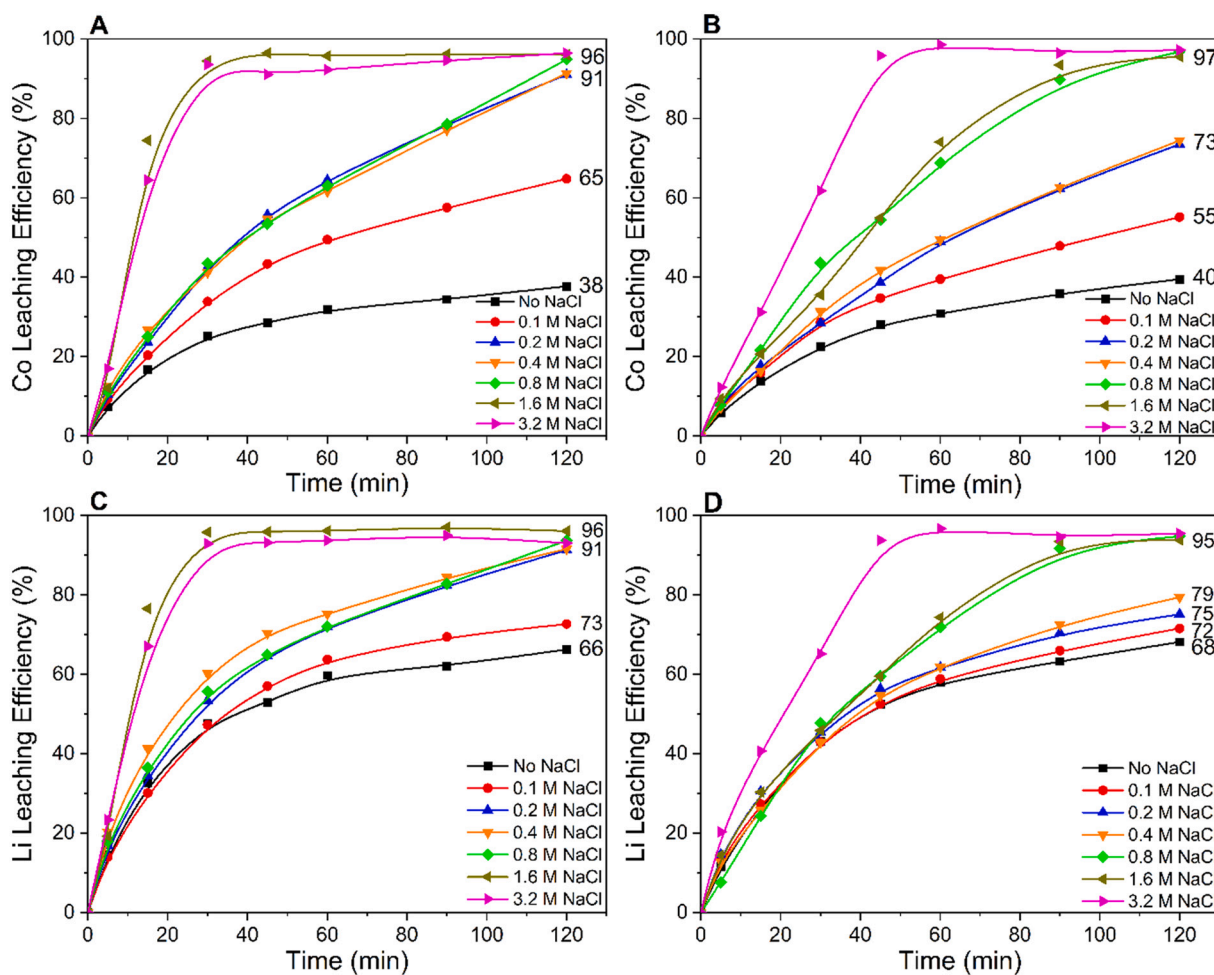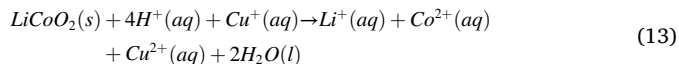

Fig. 1. Leaching efficiencies of Co at 30 °C in (A): 1 M H_2SO_4, (B): 0.5 M H_2SO_4, and Li at 30 °C in (C): 1 M H_2SO_4, (D): 0.5 M H_2SO_4. Final leaching efficiency values (%) are shown next to their respective curves.

species are subsequently reduced back to Cu^+ in the presence of solid Cu (Eq. 14). **N.B.** Both equations treat the dissolved copper species as their respective ions, without considering the effects of complexation with chloride ions.

$$LiCoO_2(s) + 4H^+(aq) + Cu^+(aq) \rightarrow Li^+(aq) + Co^{2+}(aq) \tag{13}$$
$$+ Cu^{2+}(aq) + 2H_2O(l)$$

$$Cu^{2+}(aq) + Cu(s) \rightarrow 2Cu^+(aq) \tag{14}$$

In order to study the leaching behavior in more detail, leach residues from the experiments were analyzed with XRD. The related diffractograms for 1 M (Fig. 2) and 0.5 M H_2SO_4 (Fig. 3) are displayed, along with the original LCO material, included for comparison. At low NaCl concentrations, it was found that the leach residues consist mostly of undissolved LCO and Cu. The diffractograms show the presence of $Li_{0.51}CoO_2$ after leaching without NaCl addition, which confirms that in the absence of effective reduction via Cu-facilitated electron transfer, the dissolution of LCO occurs via delithiation (Takacova et al., 2016). Delithiated LCO was also present in most residues from the experiments with 0.1–0.4 M NaCl, whereas LCO in the residues from 0.8–3.2 M NaCl was still in its stoichiometric composition, $LiCoO_2$.

In addition to undissolved LCO and Cu, most leach residues from 0.2–3.2 M NaCl contained solid CuCl – the presence of which was particularly clear in residues with 0.2–0.8 M NaCl, as it tended to precipitate on the surface of the Cu powder, forming visible clusters (Fig. S2). This precipitation could explain why the leaching efficiencies (Fig. 1) did not increase in conjunction with the chloride concentration between 0.2 and 0.8 M, as the formed CuCl layer is suggested to act as a barrier for electron transfer between Cu and LCO, limiting the reaction rate. Conversely, at chloride concentrations of $\geq$1.6 M, almost all LCO dissolved (> 90%), and the diffractograms primarily show the presence of undissolved Cu, precipitated CuCl, and residual traces of LCO. Although, CuCl was also present in these leach residues, it did not inhibit the reaction rate or formation of agglomerates.

The adverse effects of CuCl precipitation on Cu dissolution have also been investigated previously. For example, Herreros et al. (2005) observed formation of CuCl on the surface of Cu in chloride leaching and found that precipitation occurred at molar ratios Cl/Cu^{2+} of approximately $\leq$8, thereby hindering the dissolution of Cu. They suggested that under these conditions, dissolution of Cu occurs via formation of an intermediate CuCl phase (Eqs. 15 and 16).

$$Cu(s) + Cu^{2+}(aq) + 2Cl^-(aq) \rightarrow 2CuCl(s) \tag{15}$$

$$CuCl(s) + Cl^-(aq) \rightarrow CuCl_2^-(aq) \tag{16}$$
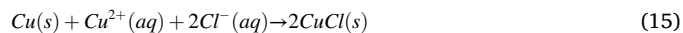
In contrast, the experiments detailed here used 0.07 mol Cu in 400 mL of lixiviant, resulting in a theoretical maximum CuCl concentration of 0.175 mol/L. Solubility calculations previously undertaken by Fritz (1982) indicate that the dissolution of this amount of CuCl would require a NaCl solution concentration of at least 1.5 M (at 30 °C), which explains why CuCl precipitation did not seem to inhibit the leaching process in experiments with $\geq$1.6 M NaCl.

3.2. Cu consumption and efficiency

In addition to improving the dissolution of Co and Li, higher chloride concentrations were also shown to increase Cu consumption (Fig. 4). In the absence of NaCl, Cu^+ ion instability leads to a situation where the reductive power of copper is negligible, and only very low levels of consumption (~5%) can be observed. The Cu dissolution that occurs is probably due to formation of oxygen (Eq. 1), which transforms Cu directly to Cu^{2+} (Eq. 5) rather than via a cuprous ion intermediate – a mechanism that has previously been shown not to enhance the dissolution of LCO (Porvali et al., 2020a). When chloride ions are added to the leaching solution, the consumption of Cu follows a trend analogous to the leaching efficiencies of Li and Co. Small increases in NaCl concentration accelerate the consumption of Cu, and a major increase in kinetics and consumptions is observed at NaCl concentrations $\geq$1.6 M. Furthermore, most experiments carried out at 1 M H_2SO_4 were found to
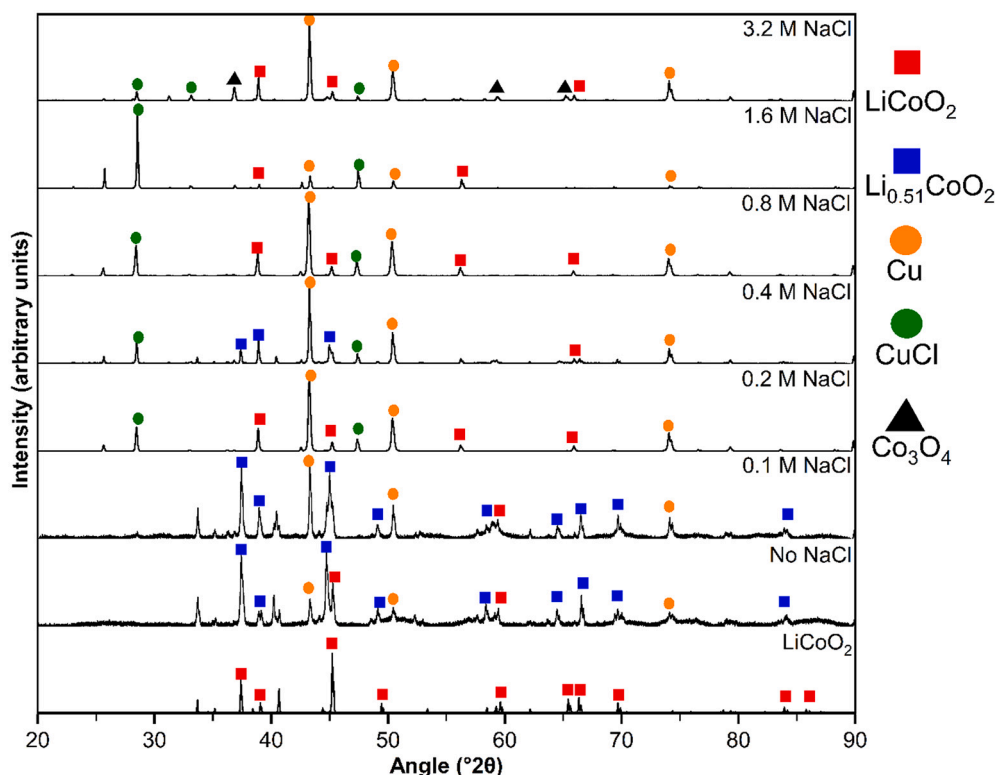
Fig. 2. XRD diffractograms of pure $LiCoO_2$ and leach residues from 1 M H_2SO_4 leaching experiments.
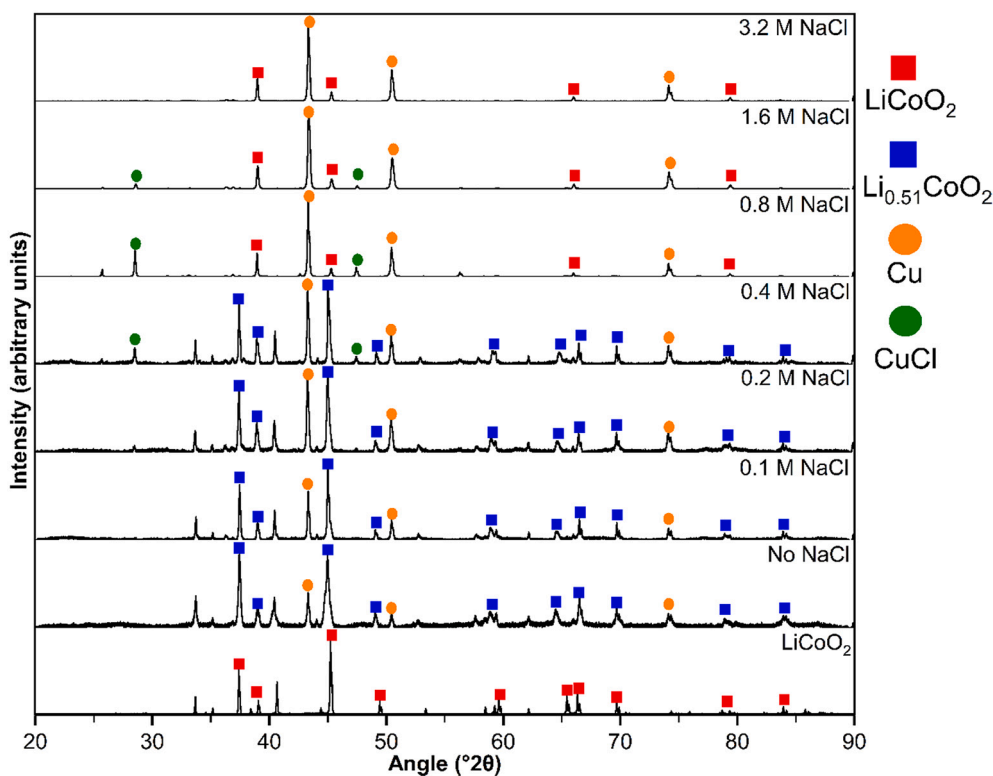
Fig. 3. XRD diffractograms of pure $LiCoO_2$ and leach residues from 0.5 M H_2SO_4 leaching experiments.
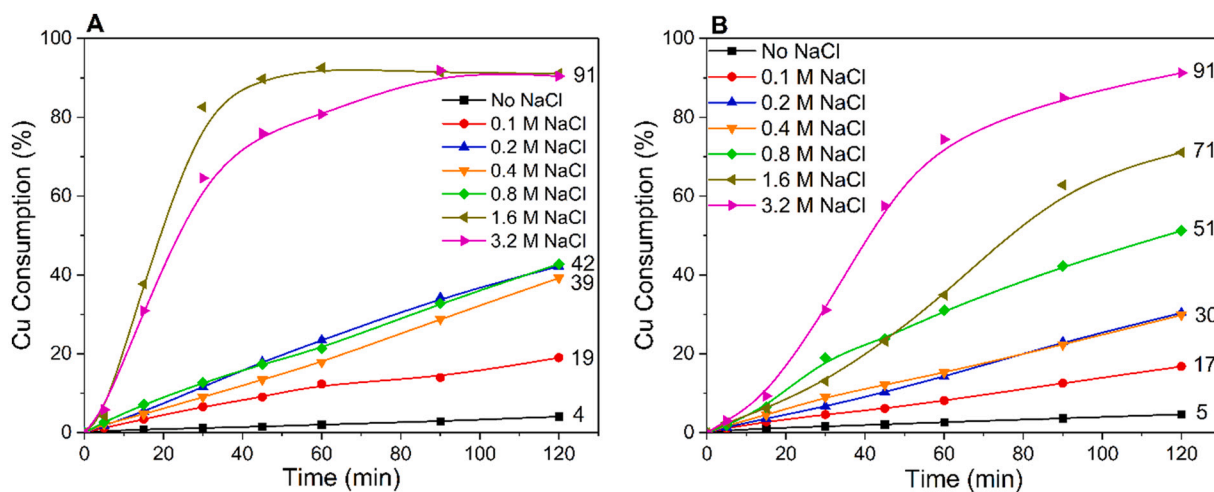

Fig. 4. Consumption of Cu at 30 °C in (A): 1 M H_2SO_4, (B): 0.5 M H_2SO_4.

consume slightly more Cu than those performed at 0.5 M H_2SO_4.

At chloride concentrations ≤0.8 M, the consumption of Cu per dissolved Co is in most cases lower than the stoichiometric ratio predicted (0.5 mol/mol, Eqs. 13 and 14), implying a higher reductive efficiency of Cu in the system, as highlighted by Fig. 5. This results from a direct reaction of LCO with the acid (Eq. 1), which allows some of the LCO to dissolve without the involvement of Cu-facilitated electron transfer. This behavior is especially clear during the initial stages when LCO is still in a more easily soluble form and the amount of monovalent copper species available for reduction is low. In contrast, at high chloride concentrations (≥ 1.6 M), the consumption of Cu per Co is higher than the stoichiometric ratio, reaching values between 0.60 and 0.88 when LCO has almost completely dissolved.

These results suggest that copper has the highest reductive efficiency

at moderate chloride concentrations (0.2–0.8 M) where Co dissolution is high (91–95% in 1 M H_2SO_4 and 73–97% in 0.5 M H_2SO_4), and no excess Cu consumption occurs. The highest efficiency in terms of Cu/Co ratio is observed at the lowest chloride concentration (0.1 M), however, the leaching kinetics are considerably slower, resulting in only 55–65% Co dissolution after 2 h (Fig. 1A and B).

Overconsumption of copper in ≥1.6 M Cl^- can be explained by the difference in the mechanism of Cu dissolution at different chloride concentrations. At lower Cl^- concentrations, Cu dissolution proceeds via precipitation of CuCl (Eqs. 15 and 16; Herreros et al., 2005), which causes the production of Cu^+ species to be slow, whilst the reaction between Cu^+ and LCO (Eq. 13) is fast. As a result, Cu dissolution is the rate-limiting step in the system, and all available Cu^+ species are quickly oxidized to Cu^{2+}. Conversely, at high chloride concentrations, CuCl
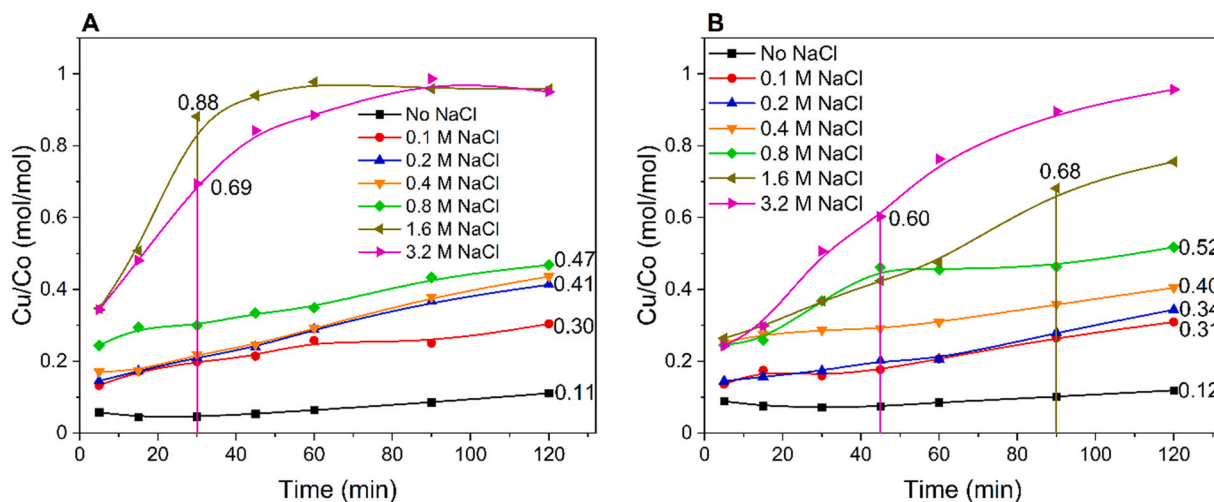
Fig. 5. Consumption of Cu per dissolved Co at 30 °C in (A): 1 M H_2SO_4, (B): 0.5 M H_2SO_4. Final consumption values (mol/mol) are shown next to their respective curves. The drop-down lines indicate the timepoints at which nearly complete dissolution of LCO was achieved.

precipitation does not limit Cu dissolution, causing the formation of Cu^+ species to be rapid. Moreover, each mole of Cu^{2+} generates 2 mol of Cu^+ (Eq. 14), whereas each mole of LCO consumes only 1 mol of Cu^+ (Eq. 13), which makes LCO dissolution the rate-limiting step. As a result, Cu dissolution is faster than that of LCO, resulting in overproduction of Cu^+ species and high Cu consumption.

3.3. Reaction rates

The reaction rates of Co dissolution in the H_2SO_4–NaCl–Cu system were investigated in NaCl concentrations of 0–3.2 M and H_2SO_4 concentrations of 1 M and 0.5 M. Based on the assumption that dissolution proceeds according to a shrinking particle model controlled by the rate of chemical reaction, the leaching reactions can be described using Eq. 17 (Levenspiel, 1998).

$$\frac{t}{\tau} = 1 - (1 - x)^{\frac{1}{3}} \tag{17}$$

where t is time (min), τ is the time required for complete conversion (min), and x is the dissolved fraction of the investigated substance (0–1). Replacing τ with the inverse of k_c, $1/k_c$, yields Eq. 18:

$$k_c \bullet t = 1 - (1 - x)^{\frac{1}{3}} \tag{18}$$

where k_c is the apparent rate constant (min^{-1}).

Fig. 6 shows the results of Co dissolution in 1 M and 0.5 M H_2SO_4 fitted to Eq. 18. For experiments where LCO was fully depleted before the end of the experimental duration (2 h), trendlines are fitted only for the part of the experiments where dissolution was still ongoing.

A majority of the experiments were determined to have followed the chemical reaction-controlled equation, with p-values below 0.05, and R^2 values between 0.965 and 0.998, indicating a good fit. Experiments without NaCl had lower R^2 values due to possible formation of more insoluble Co_3O_4 (Ferreira et al., 2009) and associated reduction in dissolution rate. Consequently, it can be said that dissolution occurring during these experiments was not completely chemical reaction controlled for the whole duration. In addition, experiments with 0.1 M NaCl were found to have R^2 values close to 0.95, which signifies a less than optimal fit. This finding probably results from a lack of Cu^+ ion availability within the solution, which causes the system to be unable to maintain the initial reaction rate between H_2SO_4 and LCO.

Results from 0 M and 0.1 M NaCl experiments were subsequently fitted to various other reaction models, however, only a diffusion-
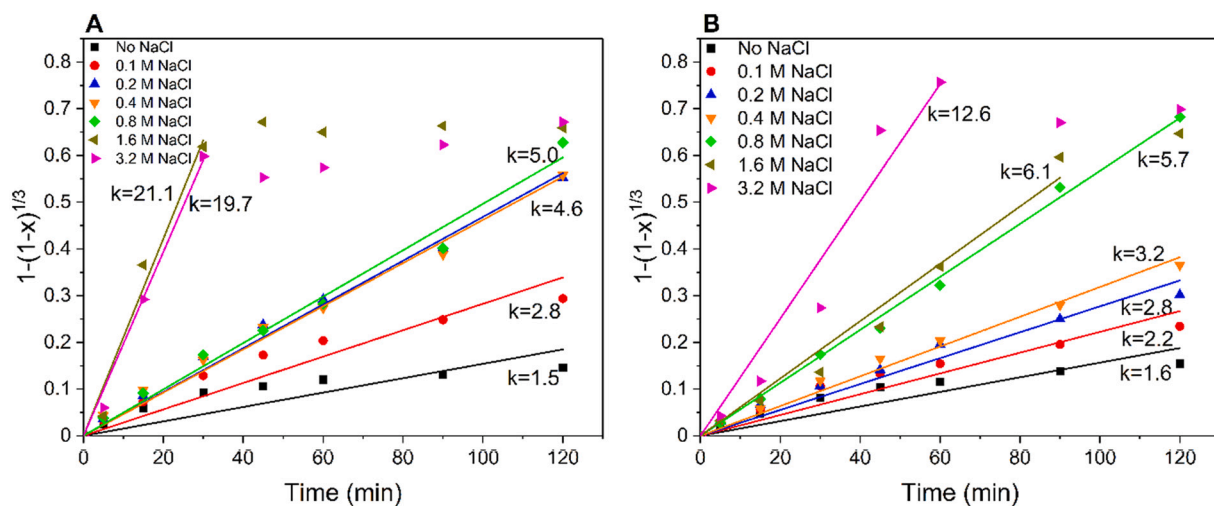

Fig. 6. Reaction rates of Co dissolution at 30 °C in (A): 1 M H_2SO_4, (B): 0.5 M H_2SO_4. Reaction rates of the experiments are shown next to their corresponding trendlines, reported as 10^{-3} min^{-1}.

controlled shrinking core model shown in Eq. 19 (Free, 2013) resulted in a good fit with R^2 values between 0.975 and 0.998. This suggests that at low Cl^- concentrations, dissolution of LCO proceeds via formation of Co_3O_4 which causes the reaction to occur according to a diffusion-controlled shrinking core model rather than a shrinking particle model. More details about calculated R^2 and p-values can be found in the Supplementary material (Tables S1–S3).

$$1 - \frac{2}{3}x - (1-x)^{\frac{2}{3}} = k_c \cdot t \qquad (19)$$

In both acid concentrations investigated, the experiments without NaCl exhibited the lowest rate constant ($k_c \approx 1.5 \times 10^{-3}$ min^{-1}), whereas the fastest reactions ($k_c > 19 \times 10^{-3}$ min^{-1}) were observed for the tests with 1.6 M and 3.2 M chloride concentrations and 1 M H_2SO_4. With 1 M H_2SO_4, formation of CuCl caused the reaction rates to stagnate at intermediate NaCl concentrations of 0.2–0.8 M, and the corresponding k_c values vary between 4.6×10^{-3}–5.0×10^{-3} min^{-1}. Despite some reaction inhibition due to the presence of CuCl, these values are very close to those previously obtained by Porvali et al. (2020b), who reported rate constants of $\sim 4.7 \times 10^{-3}$ min^{-1} in 1 M H_2SO_4 using Fe^{2+}/Fe^{3+} (~ 0.5 g/L Fe) as catalyst and Cu as reductant. With 0.5 M H_2SO_4, the effect of precipitated CuCl was not as apparent, and there are two distinct increases in rate constant, first at 0.4–0.8 M NaCl, and later at 1.6–3.2 M NaCl.

4. Conclusions

In this study, it was shown that Cu^+ species can be used as effective catalysts for electron transfer between LCO and solid Cu during sulfuric acid leaching by stabilizing them with additions of chloride ions. Using this H_2SO_4–NaCl–Cu leaching system, over 90% of Co and Li were leached in 2 h under relatively mild conditions of 1 M H_2SO_4, 0.2 M NaCl, 30 °C, thus providing an environmentally attractive alternative to traditional processes which often employ high temperatures and highly concentrated acids along with external reductants such as H_2O_2. The leaching system was also shown to be functional with a lower H_2SO_4 concentration of 0.5 M. Although, the reaction rates were generally lower than with 1 M H_2SO_4, using a lower acidity lixiviant has additional environmental benefits by producing a less acidic leach solution that requires less chemicals in the neutralization step of the recycling process.

The XRD analyses of leach residues revealed that solid CuCl precipitated on the surface of Cu during leaching. Formation of CuCl was found to hinder the dissolution of both Cu and LCO especially with 1 M H_2SO_4, as neither the leaching efficiencies nor reaction rates increased notably between 0.2 and 0.8 M NaCl. However, despite this phenomenon, reaction rates observed under these conditions were equally fast as those obtained in a previously studied Fe^{2+}-catalyzed leaching system (Porvali et al., 2020b). The inhibiting effect of CuCl precipitation was found to be minimal at NaCl concentrations of ≥ 1.6 M, which allowed for very fast reaction kinetics – almost complete dissolution of LCO was achieved in only 30 min. Nevertheless, such high chloride concentrations also increased the consumption of Cu considerably, and the presence of such a high concentration of Na, Cl, and Cu in the resulting leach solution could cause additional challenges in the form of a highly corrosive environment and added burden on subsequent downstream processes like metals recovery and solution purification.

One of the limitations of the current study is that it focused only on leaching of pure LCO, therefore, further research is required to validate the results also for a broader range of cathode materials like NMC ($LiNi_xMn_yCo_zO_2$) and NCA ($LiNi_xCo_yAl_zO_2$). Additionally, the system needs to be studied with industrially produced battery waste to confirm its applicability under current battery recycling conditions where the presence of various impurities and metallic particles can also have an impact on the overall dissolution process.

Declaration of Competing Interest

The authors declare that they have no known competing financial interests or personal relationships that could have appeared to influence the work reported in this paper.

Appendix A. Supplementary data

Supplementary data to this article can be found online at https://doi.org/10.1016/j.hydromet.2021.105808.

References

Blengini, G.A., El Latunussa, C., Eynard, U., de Matos, C.T., Wittmer, D., Georgitzikis, K., Pavel, C., Carrara, S., Mancini, L., Unguru, M., Blagoeva, D., Mathieux, F., Pennington, D., 2020. Study on the EU's List of Critical Raw Materials (2020): Final Report. European Commission. https://doi.org/10.2873/11619

Chen, X., Guo, C., Ma, H., Li, J., Zhou, T., Cao, L., Kang, D., 2018. Organic reductants based leaching: a sustainable process for the recovery of valuable metals from spent lithium ion batteries. Waste Manag. 75, 459–468. https://doi.org/10.1016/j.wasman.2018.01.021.

Chen, Y., Chang, D., Liu, N., Hu, F., Peng, C., Zhou, X., He, J., Jie, Y., Wang, H., Wilson, B.P., Lundström, M., 2019. Biomass-assisted reductive leaching in H_2SO_4 medium for the recovery of valuable metals from spent mixed-type lithium-ion batteries. JOM 71, 4465–4472. https://doi.org/10.1007/s11837-019-03775-3.

Chernyaev, A., Partinen, J., Klemettinen, L., Wilson, B.P., Jokilaakso, A., Lundström, M., 2021. The efficiency of scrap Cu and Al current collector materials as reductants in LIB waste leaching. Hydrometallurgy 203, 105608. https://doi.org/10.1016/j.hydromet.2021.105608.

European Commission, 2021. Batteries Europe raw materials and recycling roadmap. https://ec.europa.eu/energy/topics/technology-and-innovation/batteries-europe/news-articles-and-publications/batteries-europe-raw-materials-and-recycling-roadmap.

Ferreira, D.A., Prados, L.M.Z., Majuste, D., Mansur, M.B., 2009. Hydrometallurgical separation of aluminium, cobalt, copper and lithium from spent Li-ion batteries. J. Power Sources 187, 238–246. https://doi.org/10.1016/j.jpowsour.2008.10.077.

Free, M.L., 2013. Hydrometallurgy: Fundamentals and Applications. Wiley, 458 pages. ISBN: 1-118-73258-8.

Fritz, J.J., 1980. Chloride complexes of CuCl in aqueous solution. J. Phys. Chem. 84, 2241–2246. https://doi.org/10.1021/j100455a006.

Fritz, J.J., 1982. Solubility of cuprous chloride in various soluble aqueous chlorides. J. Chem. Eng. Data 27, 188–193. https://doi.org/10.1021/je00028a027.

Greenwood, N.N., Earnshaw, A., 1997. Chemistry of the Elements, Butterworth-Heinemann, 2nd edition, p. 1194. ISBN: 978-0-0805-0109-3.

Harper, G., Sommerville, R., Kendrick, E., Driscoll, L., Slater, P., Stolkin, R., Walton, A., Christensen, P., Heidrich, O., Lambert, S., Abbott, A., Ryder, K., Gaines, L., Anderson, P., 2019. Recycling lithium-ion batteries from electric vehicles. Nature 575, 75–86. https://doi.org/10.1038/s41586-019-1682-5.

Hashemzadeh, M., Dixon, D.G., Liu, W., 2019. Modelling the kinetics of chalcocite leaching in acidified cupric chloride media under fully controlled pH and potential. Hydrometallurgy 189, 105114. https://doi.org/10.1016/j.hydromet.2019.105114.

Herreros, O., Quiroz, R., Restovic, A., Viñals, J., 2005. Dissolution kinetics of metallic copper with CuSO4–NaCl–HCl. Hydrometallurgy 77, 183–190. https://doi.org/10.1016/j.hydromet.2004.11.010.

IEA, 2020. Global EV Outlook 2020. IEA, Paris. https://www.iea.org/reports/global-ev-outlook-2020.

Joulié, M., Billy, E., Laucournet, R., Meyer, D., 2017. Current collectors as reducing agent to dissolve active materials of positive electrodes from Li-ion battery wastes. Hydrometallurgy 169, 426–432. https://doi.org/10.1016/j.hydromet.2017.02.010.

Levenspiel, O., 1998. Chemical Reaction Engineering, John Wiley & Sons, 3rd edition, pp. 575–579. ISBN: 978-0-471-25424-9.

Liu, F., Peng, C., Porvali, A., Wang, Z., Wilson, B.P., Lundström, M., 2019. Synergistic recovery of valuable metals from spent nickel–metal hydride batteries and Lithium-ion batteries. ACS Sustain. Chem. Eng. https://doi.org/10.1021/acssuschemeng.

Lundström, M., Aromaa, J., Forsén, O., Hyvärinen, O., Barker, M.H., 2005. Leaching of chalcopyrite in cupric chloride solution. Hydrometallurgy 77, 89–95. https://doi.org/10.1016/j.hydromet.2004.10.013.

Lv, W., Wang, Z., Cao, H., Sun, Y., Zhang, Y., Sun, Z., 2018a. A critical review and analysis on the recycling of spent Lithium-ion batteries. ACS Sustain. Chem. Eng. 6, 1504–1521. https://doi.org/10.1021/acssuschemeng.7b03811.

Lv, W., Wang, Z., Cao, H., Zheng, X., Jin, W., Zhang, Y., Sun, Z., 2018b. A sustainable process for metal recycling from spent lithium-ion batteries using ammonium

chloride. Waste Manag. 79, 545–553. https://doi.org/10.1016/j. wasman.2018.08.027.

Metso Outotec, 2018. HSC Chemistry. https://www.mogroup.com/portfolio/hsc-ch emistry/?r=2.

Muir, D.M., 2002. Basic Principles of Chloride Hydrometallurgy, Chloride Metallurgy 2002: Practice and Theory of Chloride/Metal Interaction, Montreal, vol 2, pp. 759–791 procite:1d199478-fb25-4be4-b959-61203dcfe1d4.

Nan, J., Han, D., Zuo, X., 2005. Recovery of metal values from spent lithium-ion batteries with chemical deposition and solvent extraction. J. Power Sources 152, 278–284. https://doi.org/10.1016/j.jpowsour.2005.03.134.

Ordoñez, J., Cago, E.J., Girard, A., 2016. Processes and technologies for the recycling and recovery of spent lithium-ion batteries. Renew. Sust. Energ. Rev. 60, 195–205. https://doi.org/10.1016/j.rser.2015.12.363.

Peng, C., Liu, F., Aji, A.T., Wilson, B.P., Lundström, M., 2019. Extraction of Li and co from industrially produced Li-ion battery waste – using the reductive power of waste itself. Waste Manag. 95, 604–611. https://doi.org/10.1016/j.wasman.2019.06.048.

Porvali, A., Aaltonen, M., Ojanen, S., Velazquez-Martinez, O., Eronen, E., Liu, F., Wilson, B.P., Serna-Guerrero, R., Lundström, M., 2019. Mechanical and hydrometallurgical processes in HCl media for the recycling of valuable metals from Li-ion battery waste. Resour. Conserv. Recycl. 142, 257–266. https://doi.org/10.1016/j.resconrec.2018.11.023.

Porvali, A., Chernyaev, A., Shukla, S., Lundström, M., 2020a. Lithium ion battery active material dissolution kinetics in Fe(II)/Fe(III) catalyzed cu-H$_2$SO$_4$ leaching system. Sep. Purif. Technol. 236, 116305 https://doi.org/10.1016/j.seppur.2019.116305.

Porvali, A., Shukla, S., Lundström, M., 2020b. Low-acid leaching of lithium-ion battery active materials in Fe-catalyzed Cu-H$_2$SO$_4$ system. Hydrometallurgy 195, 105408. https://doi.org/10.1016/j.hydromet.2020.105408.

Seisko, S., Aromaa, J., Lundström, M., 2019. Features affecting the cupric chloride leaching of gold. Miner. Eng. 137, 94–101. https://doi.org/10.1016/j.mineng.2019.03.030.

Senanayake, G., 2007. Chloride assisted leaching of chalcocite by oxygenated sulphuric acid via Cu(II)–OH–Cl. Miner. Eng. 20, 1075–1088. https://doi.org/10.1016/j.mineng.2007.04.002.

Sohn, J., Shin, S., Yang, D., Kim, S., Lee, C., 2006. Comparison of two acidic leaching processes for selecting the effective recycle process of spent lithium ion battery. Geosyst. Eng. 9, 1–6. https://doi.org/10.1080/12269328.2006.10541246.

Takacova, Z., Havlik, T., Kukurugya, F., Orac, D., 2016. Cobalt and lithium recovery from active mass of spent Li-ion batteries: theoretical and experimental approach. Hydrometallurgy 163, 9–17. https://doi.org/10.1016/j.hydromet.2016.03.007.

Yao, Y., Zhu, M., Zhao, Z., Tong, B., Fan, Y., Hua, Z., 2018. Hydrometallurgical processes for recycling spent Lithium-ion batteries: a critical review. ACS Sustain. Chem. Eng. 6, 13611–13627. https://doi.org/10.1021/acssuschemeng.8b03545.

Zhang, X., Li, L., Fan, E., Xue, Q., Bian, Y., Wu, F., Chen, R., 2018. Toward sustainable and systematic recycling of spent rechargeable batteries. Chem. Soc. Rev. 47, 7239–7302. https://doi.org/10.1039/C8CS00297E.

Zhao, H., Chang, J., Boika, A., Bard, A., 2013. Electrochemistry of high concentration copper chloride complexes. Anal. Chem. 85, 7696–7703. https://doi.org/10.1021/ac4016769.

Zheng, X., Gao, W., Zhang, X., He, M., Lin, X., Cao, H., Zhang, Y., Sun, Z., 2017. Spent lithium-ion battery recycling – reductive ammonia leaching of metals from cathode scrap by sodium sulphite. Waste Manag. 60, 680–688. https://doi.org/10.1016/j.wasman.2016.12.007.